Creep Resistant Polymer Nanocomposites Reinforced with Multiwalled Carbon Nanotubes

Jinglei Yang, Zhong Zhang,* Klaus Friedrich, Alois K. Schlarb

Poly(propylene) (PP) nanocomposites filled with shorter- and longer-aspect-ratio multiwalled carbon nanotubes (MWNTs) were compounded using a twin-screw extruder and an injection moulding machine. It is shown that with only 1 vol.-% of MWNTs, creep resistance of PP can be significantly improved with reduced creep deformation and creep rate at a long-term loading period. Additionally, the creep lifetime of the nanocomposites has been considerably extended by 1 000% compared to that of a neat PP. Three possible mechanisms of load transfer were considered that could contribute to the observed enhancement of creep resistance, which are: (1) fairly good interfacial strength between MWNTs and polymer matrix, (2) increasing immobility of amorphous regions due to nanotubes acting as restriction sites, and (3) high aspect ratio of MWNTs. DSC results showing crystallinity changes in the specimens before and after creep deformation present evidence to confirm these mechanisms. Our results should lead to improved grades of creep resistant polymer nanocomposites for engineering applications.

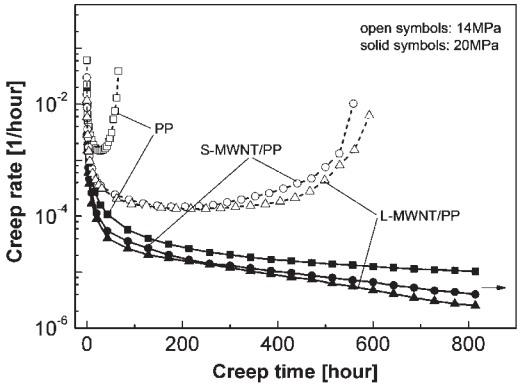

Introduction

Creep, as a time-dependent mechanism of plastic deformation, is a very important and necessary consideration for materials design in long-term durability and reliability.

J. Yang, K. Friedrich, A. K. Schlarb
Institute for Composite Materials, University of Kaiserslautern, 67663 Kaiserslautern, Germany
Z. Zhang
National Center for Nanoscience and Technology of China, 100080 Beijing, China
E-mail: zhong.zhang@nanoctr.cn
J. Yang
Current address: Beckman Institute for Advanced Science and Technology, University of Illinois at Urbana-Champaign, Urbana, IL 61801, USA

Creep performance of traditional plastic materials, such as polyamide (PA), polyethylene (PE), and poly(propylene) (PP), etc., as well as their composites, has been comprehensively studied in the past years.[1,2] With the rapid development of nanotechnologies and nanomaterials since 1990s, the studies on polymer-based nanocomposites have been extensively carried out in order to find their promising alternatives with traditional composites, though mainly focused on general mechanical and multifunctional properties and filler dispersion.[3,4] Taneike[5] reported that nanocarbonitride dispersions contributed greatly to creep lifetime prolongation and creep rate reduction in steel. However, there are only few literature concerning creep resistance of polymer nanocomposites.[6–8] Consequently, there remains the need to elaborately observe the creep performance of polymer

DOI: 10.1002/marc.200600866

nanocomposites for potential engineering applications, where the creep resistance has to be seriously considered.

Carbon nanotubes (CNTs) have greatly attracted researchers' interest since their discovery in 1991[9] due to their excellent mechanical and physical properties,[10,11] such as extremely high strength and Young's modulus compared to those of traditional carbon fibers,[12,13] making them as a much promising kind of reinforcing candidates in composites, especially in polymer matrices.[3,10,14] Great effort[14–17] has been made to develop advanced engineering materials with enhanced or novel properties by the addition of CNTs into different matrices. Several research groups have reported that the efficiency of load transfer between nanotubes and polymer chains is a critical factor to influence the resulting mechanical performance of such composite systems.[14,18–22] It is, therefore, believed that the load transfer will give rise to excellent creep resistance in nanocomposites. This enhancement is reasonably related to some nanoeffects of the CNTs, such as their high aspect ratio and large interfacial area, which can form a huge interphase between tubes and matrix and thus contribute positively to the load transfer. Previous experiments have shown some interesting results on creep resistance of nanoparticles[6,8] and layered silicate[7] filled PA composites. Recently, Suhr et al.[23] have provided enhanced viscoelastic properties of CNT/epoxy thin film, which is related to creep. Here, we report a direct creep observation of PP composites reinforced by MWNTs with different aspect ratios to characterize the long-term performance in terms of creep deformation, creep rate, and lifetime to failure.

Experimental Part

Materials and Preparation of Nanocomposites

A commercial grade of PP (Moplen HP501H, Basell Company) was considered as matrix. Larger and smaller aspect ratios of multiwalled carbon nanotubes (L-MWNTs were 5 ~ 15 μm in length, and S-MWNTs were 1 ~ 2 μm in length, supplied by Shenzhen Nanotech Port Co. Ltd., China) with outer diameter of 10 ~ 30 nm were applied as reinforcements. The volume content was in the range of 1% (1.58% by weight). The as-received matrix and nanotubes were compounded by using a Bersdoff twin-screw-extruder. In order to precisely control the filler content, commercial K-Tron weight-controlled feeders were applied during compounding. The composite granulates were finally manufactured by using an Arburg All-rounder injection moulding machine as the dog-bone tensile specimens ($160 \times 10 \times 4\ mm^3$, according to the standard of DIN EN ISO 527). Characterization by transmission electron microscopy (Figure 1) of the S-MWNT/PP composite reveals a fairly good dispersion of CNTs, which may result in huge interface and thus enhance the load transfer efficiency between tubes and matrix while the material suffers from external load.

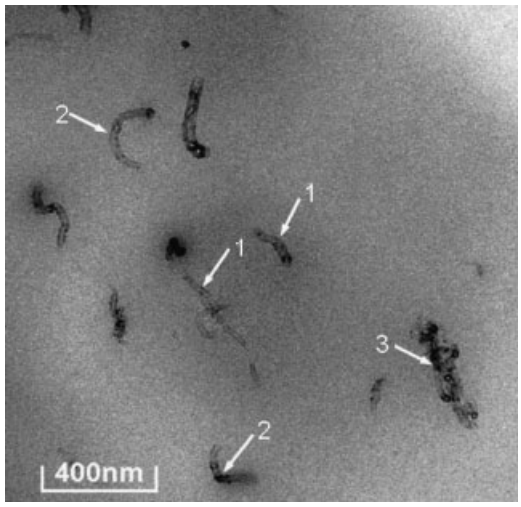

Figure 1. Transmission electron micrograph (TEM) of S-MWNT/PP composite. This TEM photograph shows a fairly well dispersion of nanotubes with different forms caused by thermal and torsional actions during melt extruding process. Arrow 1, straight tubes; arrow 2, curved tubes; and arrow 3, bundled or entangled tubes.

Static Tensile Tests and Tensile Creep Experiments

A Zwick universal testing machine (Zwick 1485) was used for uniaxial tensile testing. Both an extensometer and a 10 kN load cell were equipped for measuring tensile modulus and strength, respectively, with dog-bone tensile specimens. A gauge length of 50 mm was considered. The crosshead speed was kept constant at $2\ mm \cdot min^{-1}$ for room temperature and $5\ mm \cdot min^{-1}$ for elevated temperature (50 °C) measurements. An environmental chamber was used for high temperature testing. At least four specimens of each material were tested, and the average values with standard deviation are reported in Table 1.

The creep measurement was performed based on ASTM 2990-01 using a creep rupture test machine (Coesfeld GmbH, model 2002). Ten specimens can be measured simultaneously in an environmental chamber. For the elevated temperature measurement, the specimens in the chamber were preheated to the desired temperature for 24 h before loading in order to get a steady and uniform thermal condition. A gauge length of 30 mm was marked on each specimen, and the displacement between the marks was monitored by a video camera, which is equipped with a program-controlled step motor and connected with a computer imaging analysis system during the whole period of creep testing. The pure PP, S-, and L-MWNT/PP specimens were tested at four stress levels and two temperatures. The detailed testing conditions are listed in Table 2.

Thermal Analyses

Dynamic mechanical thermal analysis (DMTA) was carried out to determine the effects of nanofillers on the glass transition temperature (T_g). DMTA experiments were performed with rectangular specimens ($50 \times 10 \times 4\ mm^3$) under tension loading

Macromol. Rapid Commun. **2007**, *28*, 955–961

Macromolecular Journals
DOI: 10.1002/marc.200600866

Table 1. The static tensile properties of the specimens used in the present study.

Specimen	23 °C[a)]			50 °C[b)]		
	Young's modulus	Ultimate tensile strength	Strain at necking	Young's modulus	Ultimate tensile strength	Strain at necking
	MPa	MPa	%	MPa	MPa	%
PP	1 629 ± 57	30.5 ± 0.2	20.3 ± 0.8	1 047 ± 20	21.0 ± 0.2	30.4 ± 6.0
S-MWNT/PP	1 870 ± 25	33.6 ± 0.2	16.9 ± 1.1	1 239 ± 97	24.3 ± 0.3	20.5 ± 1.9
L-MWNT/PP	2 076 ± 29	34.3 ± 0.2	14.9 ± 0.7	1 304 ± 100	25.1 ± 0.2	22.6 ± 4.6

[a)]Tested at a tensile speed of 2 mm · min^{-1}; [b)]Tested at a tensile speed of 5 mm · min^{-1}.

at 10 Hz using an Eplexor 25 N device of Gabo Qualimeter. The static and cyclic (sinusoidal) loads were set as 20 and ±10 N, respectively. Temperature range of −50 to +100 °C was used. The mechanical loss factor (tan δ) was measured to determine T_g at a heating rate of 2 °C · min^{-1} for at least two samples.

A differential scanning calorimeter (Mettler Toledo, DSC 821) was used to measure the crystallinity of specimens before and after creep experiments. The temperature range of −20 to 220 °C was considered. The mass of samples was cut from bulk specimens in the range of 10–20 mg. The heating rate was set as 10 °C · min^{-1} and at least three samples were measured. Crystallinity was then calculated by the ratio of the specific melting heat of the specimens to that of the fully crystallized matrix, as given in literature.

Results and Discussion

Figure 2(a) shows the experimental data for creep strain versus time at 23 °C under 14 MPa and 20 MPa. The arrow indicates that the specimens are not a failure within the observation time scale. It can be clearly seen that the time-dependent non-deformability of the composites is significantly enhanced with reduced creep strain under both stress levels. L-MWNT/PP behaves as a slightly better creep resistance than S-MWNT/PP. Additionally, the creep lifetime of S-MWNT/PP and L-MWNT/PP is extended by about 760 and 800%, respectively, compared to that of pure matrix under 20 MPa. The reinforcing efficiency of MWNTs is confirmed at elevated temperature, as shown in Figure 2(b). The lifetime of the two composites is prolonged by 1 000% (11-fold) compared to that of pristine PP resin under 14 MPa. To qualify the time-dependent deformation and the viscoelasticity of the materials, the 1-h isochronous stress-strain data are presented in Figure 2(c) and 2(d) at 23 and 50 °C, respectively. Both at room and at elevated temperatures, the composites deform with nearly half amount of neat PP under each stress level, which indicates that the load bearing capability is greatly improved by the appearance of MWNTs. In addition, a non-linear relationship between creep strain and applied stress implies, the materials display a non-linear viscoelasticity under the observed stress range. The similarly increased linearity in the composites demonstrates that the viscous flow and mobility of the polymer chains is greatly restricted by the presence of nanotubes under each stress level. The tensile properties of the materials have been determined. Except for the reduced ductibility, Young's modulus and tensile strength of the composites are increased to some extent, as listed in Table 1.

In order to study the effect of nanotube fillers on the creep rate, the sample curves of creep rate versus time are present in Figure 3(a) (at 23 °C) and 3(b) (at 50 °C), corresponding to the creep strain in Figure 2(a) and 2(b), respectively. The complete creep rate curves consist of the primary creep region, where the creep rate decreases with

Table 2. Creep observation times (h) at each condition in the present study.

Specimen	23 °C				50 °C		
	8 MPa	11 MPa	14 MPa	20 MPa[a)]	8 MPa	11 MPa	14 MPa[a)]
PP	300	260	800	66	350	220	16.4
S-MWNT/PP	300	260	800	560	350	220	185
L-MWNT/PP	300	260	800	592	350	220	187

[a)]Advanced necking and failure occurred. Creep at other times was interrupted without occurrence of failure.

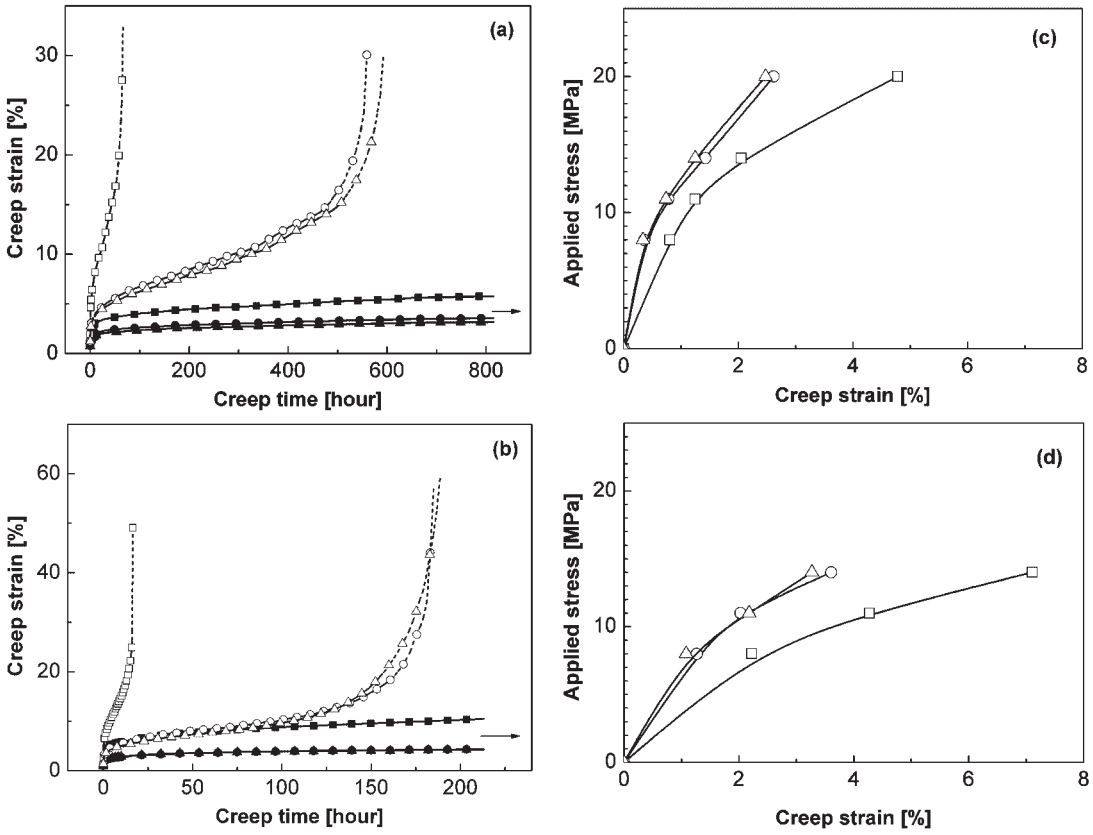

Figure 2. Experimental creep strain data. (a) Creep strain as a function of time at 23 °C under 14 MPa (solid symbols) and 20 MPa (open symbols). (b) Creep strain as a function of time at 50 °C under 11 MPa (solid symbols) and 14 MPa (open symbols). The arrows in (a) and (b) indicate, the specimens are not in failure within the observation time scale. (c) 1-h isochronous creep strain-stress relationship at 23 °C. (d) 1-h isochronous creep strain-stress relationship at 50 °C. Rectangles, PP; circles, S-MWNT/PP; triangles, L-MWNT/PP.

time, and the tertiary creep region, where the creep rate increases with time after reaching a minimum value and an accelerating creep process occurs finally with the advanced necking of material. To compare the creep rate at certain time, the creep rupture is not necessary since for the small stress cases there is no tertiary region even for a sufficient long-time observation [creep curves under 14 MPa in Figure 2(a)]. In the initiative creep stage below 0.1 h, the creep rate is nearly the same for all the specimens under the same condition. The composites thereafter display advanced decrease in creep rate with time [Figure 3(a) and 3(b)]. However, the relative magnitude of decrease in creep rate is increased with increasing stress levels. Additionally, the onset of tertiary creep is retarded up to longer times by the loading of nanotubes. This retardation leads to the longer duration of primary and secondary creep regions, which results in lower minimum creep rate and longer time to failure [Figure 3(a) and 3(b)]. Figure 3(c) and 3(d) compare the creep rates under different stress levels at 23 and 50 °C, respectively. The minimum creep rate of the materials with a tertiary creep stage and the 200-h creep rate of the materials without a tertiary creep stage in the observed time scale are plotted for comparison. The creep rate obviously increases with increasing stress level and temperature while is reduced by the appearance of nanotubes. It is noteworthy to point out that the creep rate of the nanocomposites is decreased relatively by 91 and 95% at 23 °C/20 MPa and at 50 °C/14 MPa, respectively, compared to that of baseline matrix. The aspect ratio of nanotubes in the observed range shows trivial influence in the resulting creep rate.

Three possible mechanisms of load transfer are considered that could contribute to the observed enhancement of creep resistance, which are (i) fairly good interfacial strength between MWNTs and polymer matrix, (ii) increasing immobility of amorphous region due to the appearance of nanotubes acting as blocking sites, and (iii) high aspect ratio of MWNTs. It is found from Table 1 that the Young's modulus of S- and L-MWNT/PP is increased by 15 and 27% at 23 °C, while by 18 and 25% at 50 °C, respectively, compared to that of the neat matrix. The tensile strength of S- and L-MWNT/PP is increased by 10 and 12 at 23 °C, and by 16 and 20% at 50 °C, respectively. The tensile results are coincident with those reported in the ref.,[19] indicating that the external tensile loads are successfully transferred to the nanotubes in terms of shear

Macromol. Rapid Commun. **2007**, *28*, 955–961

Macromolecular Journals
DOI: 10.1002/marc.200600866

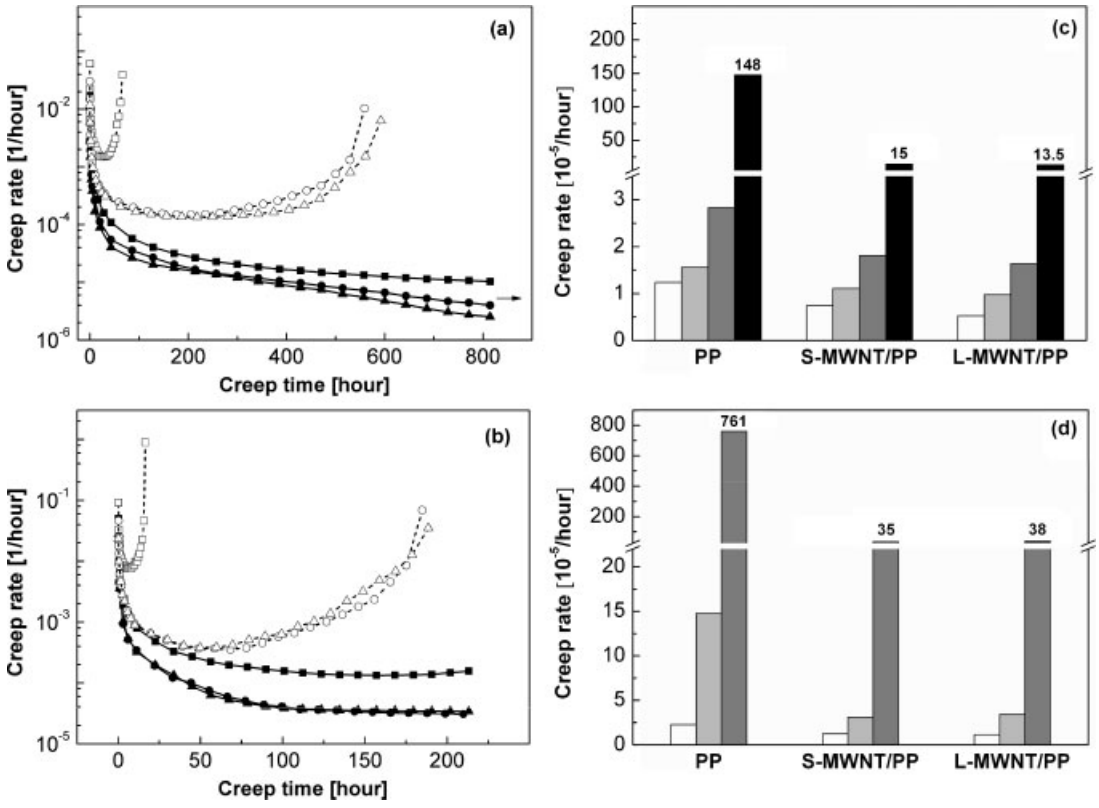

Figure 3. Experimental creep rates. (a) Creep rate as a function of time at 23 °C under 14 MPa (solid symbols) and 20 MPa (open symbols). (b) Creep rate as a function of time at 50 °C under 11 MPa (solid symbols) and 14 MPa (open symbols). Rectangles, PP; circles, S-MWNT/PP; triangles, L-MWNT/PP. (c) Creep rate versus stress level at 23 °C. (d) Creep rate versus stress level at 50 °C. White, 8 MPa; light gray, 11 MPa; gray, 14 MPa; dark gray, 20 MPa.

stress through the CNT/PP interface. A schematic deformation model under uniaxial stress is demonstrated in Figure 4. In fact, MWNTs are not ideally dispersed in PP, as represented in Figure 4(a) with some bundles or entanglements. Consequently, the existence of intertube sliding or stick-slip[23,24] may give rise to an increase in creep rate under low tensile stress, as depicted in Figure 4(b). Under high tensile stress level the large deformation of matrix may introduce high interfacial shear stress to nanotubes across good interfacial bonding. Most of the bundled tubes in the matrix will extensively slip in a short time period (compare the circled parts in Figure 4), which results in relatively high creep rate [Figure 3(c) and 3(d)]. The influence of intertube sliding becomes thereafter minor and more nanotubes are effectively transferred to sustain the external tensile load, as shown in Figure 4(c) with possible necking at matrix-rich parts thereafter. The significant reduction of creep rate and deformation is then achieved. The load-bearing capability is enhanced and the secondary creep stage is prolonged under high stress level.

Thermal analyses showed additional information of the mobility of polymer chains and crystallinity in neat PP and the nanocomposites. The T_g obtained from DMTA for the MWNTs filled PP (11.5 °C) was very close to that of neat PP (12.8 °C), showing that the addition of nanotube fillers has no significant effect on the curing properties of PP. In a non-isothermal crystallization process, crystallinity is only slightly decreased by about 1% after the addition of

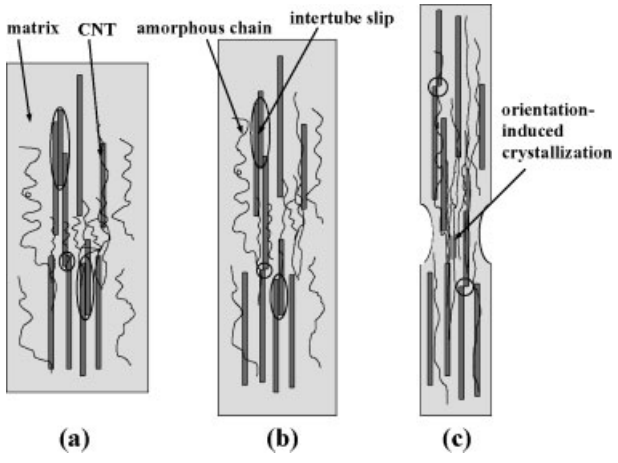

Figure 4. Schematic deformation model and orientation-induced crystallization of CNT/PP composite under uniaxial stress: (a) before loading, (b) under small load levels, and (c) under high load levels.

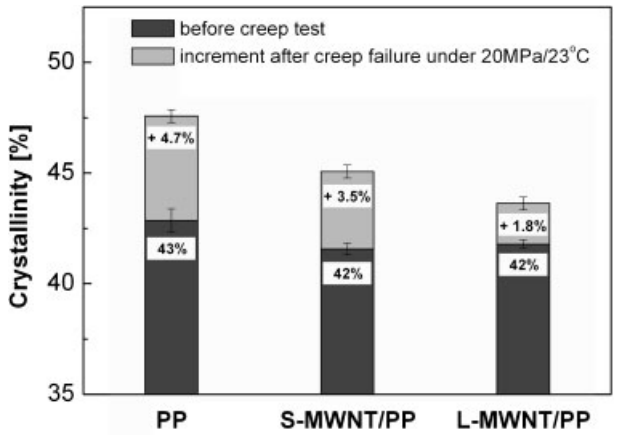

Figure 5. Changes in crystallinity of neat PP and nanotube composites before and after creep experiments under 20 MPa/23 °C. The small increase in crystallinity of L-MWNT/PP shows that the larger aspect ratio nanotubes are more capable to restrict the orientation of polymer chains than the smaller ones.

nanotubes before creep testing using DSC method, as presented in Figure 5. Some research groups[25–28] reported that CNTs might act as nucleating agent in PP at low content during isothermal crystallization process to speed both nucleating and crystallization rate and thus possibly increase the degree of crystallinity, which brings to reduced creep deformation. However, in non-isothermal crystallization, the amount of crystalline phase could be the same for the filled and unfilled samples.[26] Accordingly, in our results the effect of crystallinity change on the creep behavior is negligible. However, after creep failure, e.g., under 23 °C/20 MPa, the crystallinity is increased by 4.7% in PP while by 3.5 and 1.8% in S- and L-MWNT/PP, respectively, compared to that of the corresponding one before creep experiment. Orientation-induced crystallinity under tensile load is resulted from the permanent flow and regular rearrangement of amorphous polymer chains,[29,30] as demonstrated in Figure 4. This result implies MWNTs, especially L-MWNTs, have good capability of decreasing the mobility of amorphous polymer segments.

To understand the importance of the filler aspect ratio mechanism, it is necessary to refer to the earlier results. It is known that load transfer is most efficient if individual CNT carries the maximum saturated axial stress at its entire length. Computational work[31] has shown that under a uniaxial load, the axial stress in CNT increases from both the CNT ends and reaches to a maximum saturated value if CNT aspect ratio is sufficiently high. Their modeling results through analytical method and finite element analysis showed that the aspect ratio of CNTs is required to be larger than 400 for maximum stress transfer to occur through the CNT length. For our materials taking $l/d = 1.5\ \mu m/20\ nm = 75$ for S-MWNTs and $l/d = 10\ \mu m/20\ nm = 500$ for L-MWNTs as the aspect ratios, it is to convince accordingly that the latter have a much better load transfer efficiency. It is also referable to compare the results of traditional carbon fibers reinforced polymers. Qian et al.[19] compared their tensile results of MWNT ($l/d = 450$)/polystyrene (PS) with those of vapor-grown carbon fiber (VGCF, $l/d = 18$)/PP and a commercial high-modulus carbon fiber (E-75, $l/d = 44$)/PS composite. The filler content is the same as 0.5 vol.-%. The experimental moduli of MWNT/PS, VGFC/PP, and E-75/PS are close to the corresponding calculated values.[19] The nanocomposite is superior to fiber-composites under the same filler loading, which is considered as the contribution of their large aspect ratio. In view of these results, it seems reasonable to believe, the aspect ratio of MWNTs in our composites plays an important role in transferring load and thus enhancing the creep resistance.

It should be mentioned that the close resulting performance of S- and L-MWNT/PP nanocomposites might also result from the material processing. In the melt extrusion, the longer tubes are easy to be shortened, curved, or entangled due to the existence of thermal and torsional actions. These negative effects are responsible for the discounted results of L-MWNT/PP.

Other minor stress transfer mechanisms are possible as well, namely, that the stress is also transferred into tension through the nanotube ends[32] and curved and entangled nanotubes (Figure 1). The efficiency of this kind of load transfer mechanism is obviously lower than that of straight nanotubes parallel to the loading direction. However, it is difficult to evaluate at this point. The effects of other parameters, including wall thickness and tube diameter, on the interfacial strength and load transfer efficiency remain to be studied.

Conclusion

This study has demonstrated that the service lifetime and creep resistance of the carbon nanotube composites are significantly improved. Only 1 vol.-% MWNTs contribute to these improvements without sacrificing mechanical properties and weight penalty. A load transfer effect resulting from fairly good interfacial bonding between CNTs and matrix, CNTs acting as restriction sites, and high CNT aspect ratio are analyzed. In addition, our materials are manufactured using an industrial procedure, which could therefore greatly improve grades of creep resistant polymer nanocomposites for large scale engineering applications.

Acknowledgements: Z. Zhang is grateful to the Alexander von Humboldt Foundation for his Sofja Kovalevskaja Award (2001–2006), financed by the *German Federal Ministry of Education and Research (BMBF)* within the German Government's

DOI: 10.1002/marc.200600866

program for investment in the future, as well as a key project on "Carbon Nano-Tubes/Polymer Composites" a key item within the knowledge Innovation Projects of Chinese Academy of Sciences (Grant No. KJCX2-YW-M01).

Received: December 11, 2006; Revised: February 3, 2007; Accepted: February 7, 2007; DOI: 10.1002/marc.200600866

Keywords: carbon nanotubes; creep; load transfer; nanocomposites; poly(propylene)

[1] I. M. Ward, "*Mechanical Properties of Solid Polymers*", John Wiley & Sons, Chichester 1983.
[2] W. N. Findley, J. S. Lai, K. Onaran, "*Creep and Relaxation of Nonlinear Viscoelastic Materials*", Dover Publications Inc., New York 1989.
[3] P. M. Ajayan, L. S. Schadler, P. V. Braun, "*Nanocomposite Science and Technology*", Wiley-VCH, Weinheim 2003.
[4] L. Nicolais, G. Carotenuto, "*Metal-Polymer Nanocomposites*", John Wiley & Sons, Hoboken 2005.
[5] M. Taneike, F. Abe, K. Sawada, *Nature* **2003**, *424*, 294.
[6] Z. Zhang, J.-L. Yang, K. Friedrich, *Polymer* **2004**, *45*, 3481.
[7] D. P. N. Vlasveld, H. E. N. Bersee, S. J. Picken, *Polymer* **2005**, *46*, 12539.
[8] J.-L. Yang, Z. Zhang, A. K. Schlarb, K. Friedrich, *Polymer* **2006**, *47*, 2791.
[9] S. IIjima, *Nature* **1991**, *354*, 56.
[10] V. N. Popov, *Mater. Sci. Eng. R.* **2004**, *43*, 61.
[11] S. Reich, C. Thomsen, J. Maultzsch, "*Carbon Nanotubes*", Wiley-VCH Verlag, Weinheim 2004.
[12] K. Tanaka, T. Yamabe, K. Fukui, "*The Science and Technology of Carbon Nanotubes*", Elsevier Science Ltd, Oxford 1999.
[13] D. Qian, G. J. Wagner, W. K. Liu, M.-F. Yu, R. S. Ruoff, *Appl. Mech. Rev.* **2002**, *55*, 495.
[14] E. T. Thostenson, Z. Ren, T.-W. Chou, *Compos. Sci. Technol.* **2001**, *61*, 1899.
[15] P. M. Ajayan, L. S. Schadler, C. Giannaris, C. Rubio, *Adv. Mater.* **2000**, *12*, 750.
[16] M. Cadek, J. N. Coleman, V. Barron, K. Hedicke, W. J. Blau, *Appl. Phys. Lett.* **2002**, *81*, 5123.
[17] H. H. Ye, H. Lam, N. Titchenal, Y. Gogotsi, F. Ko, *Appl. Phys. Lett.* **2004**, *85*, 1775.
[18] L. S. Schadler, S. C. Giannaris, P. M. Ajayan, *Appl. Phys. Lett.* **1998**, *73*, 3842.
[19] D. Qian, E. C. Dickey, R. Andrews, T. Rantell, *Appl. Phys. Lett.* **2000**, *76*, 2868.
[20] A. H. Barber, S. R. Cohen, H. D. Wagner, *Appl. Phys. Lett.* **2003**, *82*, 4140.
[21] D. Qian, W. K. Liu, R. S. Ruoff, *Compos. Sci. Technol.* **2003**, *63*, 1561.
[22] C. Velasco-Santos, A. L. Martinez-Hernandez, V. M. Castano, *Compos. Interfaces* **2005**, *11*, 567.
[23] J. Suhr, N. Koratkar, P. Keblinski, P. Ajayan, *Nat. Mater.* **2005**, *4*, 134.
[24] M.-F. Yu, B. I. Yakobson, R. S. Ruoff, *J. Phys. Chem. B* **2000**, *104*, 8764.
[25] K. Lazano, E. V. Barrera, *J. Appl. Polym. Sci.* **2001**, *79*, 125.
[26] B. P. Grady, F. Pompeo, R. L. Shambaugh, D. E. Resasco, *J. Phys. Chem. B* **2002**, *106*, 5852.
[27] A. R. Bhattacharyya, T. V. Sreekumar, T. Liu, S. Kumar, L. M. Ericson, R. H. Hauge, R. E. Smalley, *Polymer* **2003**, *44*, 2373.
[28] E. Assouline, A. Lustiger, A. H. Babber, C. A. Cooper, E. Klein, E. Wachtel, H. D. Wagner, *J. Polym. Sci. B* **2003**, *41*, 520.
[29] L. Mandelkern, "*Crystallization of Polymers*", McGraw-Hill, New York 1964.
[30] I. J. Rao, K. R. Rajagopal, *Inter. J. Solids Struct.* **2001**, *38*, 1149.
[31] A. Haque, A. Ramasetty, *Compos. Struct.* **2005**, *71*, 68.
[32] H. D. Wagner, O. Lourie, Y. Feldman, R. Tenne, *Appl. Phys. Lett.* **1998**, *72*, 188.